

This is an ACCEPTED VERSION of the following published document:

Gende, M., de Moura, J., Novo, J., Ortega, M. (2022). High/Low Quality Style Transfer for Mutual Conversion of OCT Images Using Contrastive Unpaired Translation Generative Adversarial Networks. In: Sclaroff, S., Distanti, C., Leo, M., Farinella, G.M., Tombari, F. (eds) Image Analysis and Processing – ICIAP 2022. ICIAP 2022. Lecture Notes in Computer Science, vol 13231. Springer, Cham. https://doi.org/10.1007/978-3-031-06427-2_18

Link to published version: https://doi.org/10.1007/978-3-031-06427-2_18

General rights:

This version of the article has been accepted for publication, after peer review and is subject to [Springer Nature's AM terms of use](#), but is not the Version of Record and does not reflect post-acceptance improvements, or any corrections. The Version of Record is available online at: https://doi.org/10.1007/978-3-031-06427-2_18

High/Low Quality Style Transfer for Mutual Conversion of OCT Images Using Contrastive Unpaired Translation Generative Adversarial Networks*

Mateo Gende^{1,2}[0000-0003-1686-7189], Joaquim de Moura^{1,2}[0000-0002-2050-3786],
Jorge Novo^{1,2}[0000-0002-0125-3064], and Marcos Ortega^{1,2}[0000-0002-2798-0788]

¹ Centro de investigación CITIC, Universidade da Coruña, A Coruña, Spain

² Grupo VARPA, Instituto de Investigación Biomédica de A Coruña (INIBIC)
Universidade da Coruña, A Coruña, Spain

{m.gende,joaquim.demoura,jnovo,mortega}@udc.es

Abstract. Recent advances in artificial intelligence and deep learning models are contributing to the development of advanced computer-aided diagnosis (CAD) systems. In the context of medical imaging, Optical Coherence Tomography (OCT) is a valuable technique that is able to provide cross-sectional visualisations of the ocular tissue. However, OCT is constrained by a limitation between the quality of the visualisations that it can produce and the overall amount of tissue that can be analysed at once. This limitation leads to a scarcity of high quality data, a problem that is very prevalent when developing machine learning-based CAD systems intended for medical imaging. To mitigate this problem, we present a novel methodology for the unpaired conversion of OCT images acquired with a low quality extensive scanning preset into the visual style of those taken with a high quality intensive scan and vice versa. This is achieved by employing contrastive unpaired translation generative adversarial networks to convert between the visual styles of the different acquisition presets. The results we obtained in the validation experiments show that these synthetic generated images can mirror the visual features of the original ones while preserving the natural tissue texture, effectively increasing the total number of available samples that can be used to train robust machine learning-based CAD systems.

* This research was funded by Instituto de Salud Carlos III, Government of Spain, DTS18/00136 research project; Ministerio de Ciencia e Innovación y Universidades, Government of Spain, RTI2018-095894-B-I00 research project; Ministerio de Ciencia e Innovación, Government of Spain through the research project with reference PID2019-108435RB-I00; Consellería de Cultura, Educación e Universidade, Xunta de Galicia, Grupos de Referencia Competitiva, grant ref. ED431C 2020/24, predoctoral grant ref. ED481A 2021/161 and postdoctoral grant ref. ED481B 2021/059; Axencia Galega de Innovación (GAIN), Xunta de Galicia, grant ref. IN845D 2020/38; CITIC, Centro de Investigación de Galicia ref. ED431G 2019/01, receives financial support from Consellería de Educación, Universidade e Formación Profesional, Xunta de Galicia, through the ERDF (80%) and Secretaría Xeral de Universidades (20%).

Keywords: Optical Coherence Tomography · Generative Adversarial Networks · Style Transfer · Synthetic Images.

1 Introduction

According to the World Health Organisation, more than 2.2 billion people suffer from vision impairment. Of these, at least 1 billion have a condition that could have been prevented or is yet to be addressed. Conversely, a considerable proportion of people with eye conditions who receive timely diagnosis and treatment do not develop blindness [25]. This motivates the need for accurate and accessible diagnostic tools that can detect these diseases in their early stages.

Recent advances in medical imaging techniques, plus the development of new and improved machine learning algorithms, are contributing to build Computer-Aided Diagnosis (CAD) systems that can help to recognise and prevent these conditions. These algorithms allow deep learning models to be trained directly from annotated data. This greatly simplifies the development of CAD systems at the cost of requiring vast amounts of training images that, unfortunately, are not always readily available. The problem of data scarcity affects many domains of application of deep learning [20], but it is especially prevalent in medical imaging [13], due to the sensitive nature of the data and its acquisition costs.

In the context of medical imaging, Optical Coherence Tomography (OCT) is a non-invasive imaging technique that can obtain volumetric digitalisations of the tissue of the eyes. Due to its ability to visualise cross-sections of relevant pathological structures, OCT has been used extensively to diagnose ocular diseases [19, 18] such as diabetic macular edema [24] or glaucoma [23, 9]. While OCT-based diagnosis is usually performed by the clinician visually inspecting several images, this task is considerably labour-intensive and time-consuming, as well as subjective in nature.

To mitigate this problem and to aid the experts in their undertaking, many OCT-based CAD systems make use of machine learning algorithms and deep learning models [3, 15, 22], all while achieving results that are equal to or better than board-certified specialists [11, 21, 6, 13]. The functions of such systems can range from the detection and visualisation of pathological structures [5], to the segmentation and measurement of anatomical parts of the eye that are relevant for diagnosis [4] or the automatic diagnosis of patients in screening tests [3]. However, as mentioned above, the development process of these systems requires a considerable amount of data.

To obtain the images, an OCT scanner sweeps the retina of the patient via interferometry with a low coherence beam of light, obtaining samples for each point and usually creating a visualisation based on the average of said samples. The number of samples that is taken has a direct effect on the image quality, with longer scans over a smaller area of the retina providing higher quality images than those that are taken over a larger surface, while the latter allow for a wider portion of the eye to be analysed at once. To simplify the operation, manufacturers typically provide different scanning presets so that the clinicians

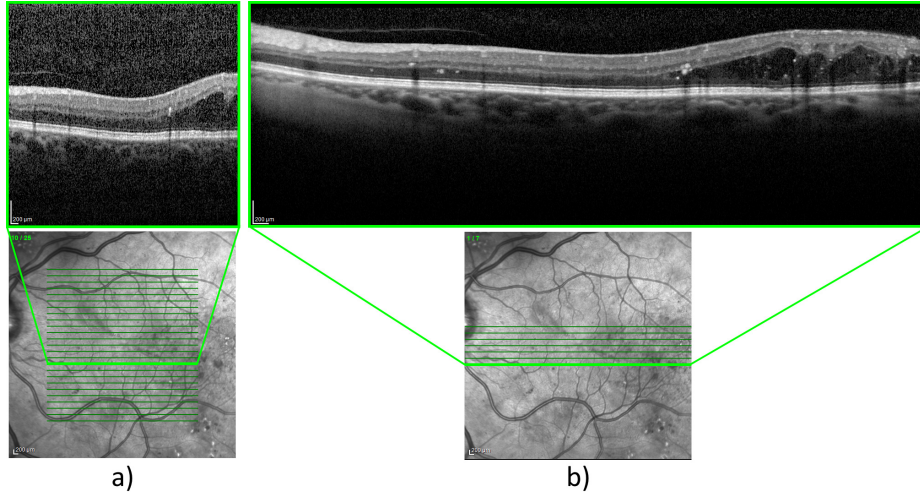


Fig. 1. Example of two slices from different scanning settings taken from the same location. a) “*Macular Cube*” preset. b) “*Seven Lines*” preset.

can choose which kind of scan they want to perform based on the needs and the condition of the patient, as well as the time they have available. This usually tends to result in either small, high-quality volumes that cover a long and narrow part of the retina or noisier, lower-resolution images that can cover most of the retina surface. Figure 1 shows an example of the two most representative scan presets used in clinical practice, displaying a “*Macular Cube*” preset where 25 OCT slices are sampled at a low rate, resulting in low resolution, noisy images of the whole retina and a “*Seven Lines*” preset where only 7 slices are sampled at a higher rate and quality over a narrow strip of tissue. These two kinds of presets are the most prevalent in medical services, reference works and publicly available datasets.

This compromise between OCT slice quality and sampled area places a limit on the amount of high quality data that can be obtained in a single session, in this way contributing to the problem of data scarcity that was mentioned above. This problem has been approached by several authors by applying super-resolution or reducing the speckle noise present in the images, for reference [8, 1, 12, 26], with varying degrees of success at enhancing the quality of extensive OCT scans. Despite these results, however, none of these works have addressed the visual differences that exist between images acquired with different scanning presets. Moreover, a machine learning system that has been trained with images acquired with a particular preset may not be able to perform as well when applied to data from another configuration due to the visual differences between images of different presets.

In this work, we present a novel fully automatic methodology to address the issue of data scarcity in OCT imaging. By making use of a Contrastive Unpaired

Translation Generative Adversarial Network (CUT-GAN) architecture, the visual style of images acquired with a superior quality preset can be transferred to data obtained with a more extensive, lower quality preset and vice versa. This way, the total number of available samples can be effectively multiplied, contributing to mitigate this problem of data scarcity that is so prevalent when developing OCT-based CAD systems. Furthermore, this methodology has the potential to create multi-preset datasets which can then be used to train CAD systems in a robust manner, without the need to obtain samples acquired with every preset the system may encounter in service. To the best of our knowledge, this proposal represents the only study designed specifically for the mutual conversion of OCT samples acquired with different scanning presets most commonly used in the health services.

2 Methodology

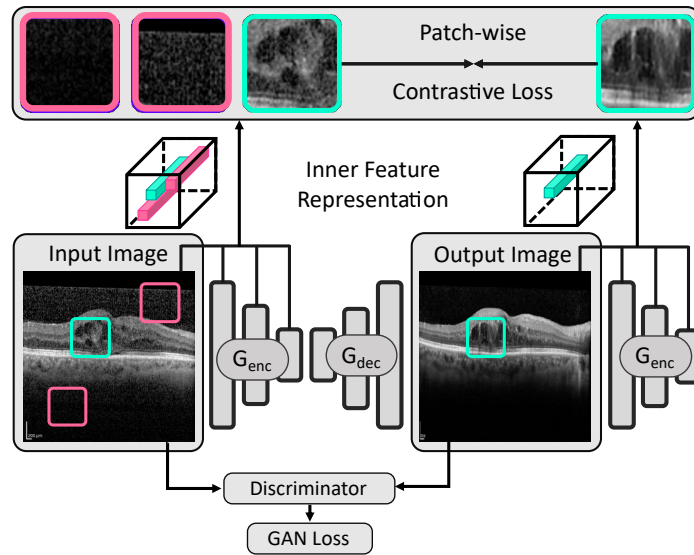


Fig. 2. Patch-wise contrastive learning for OCT images. Contrastive loss is obtained by comparing the inner representations of patches extracted from the input and output images.

To convert the images between the two scanning presets, a CUT-GAN architecture was used [17]. This architecture is able to perform unpaired image-to-image translation between two classes by training in a patch-wise manner while trying to preserve the mutual information in both input and output images. By training this architecture on our two classes corresponding to different acquisi-

tion presets, we can obtain models that are able to perform a “style transfer”, conferring the visual features of any preset to images taken with another.

This can be achieved by employing a patch-wise contrastive loss. As an image is propagated through the network, patches of its inner representation, taken as the output of the encoder part of the generative network, are compared with the inner representation of the corresponding synthetic generated image. Similar inner representations will minimise this contrastive loss. This way, we can leverage the potential of the encoder part of the network to capture features that are common to both presets, such as the choroid or the location of the inner limiting membrane, while taking advantage of the ability of the decoder part to synthesise preset-specific features such as speckle noise or detailed tissue texture. This process is illustrated in Figure 2.

For this purpose, we trained a model to make the conversion of images acquired with the “*Macular Cube*” preset into those of a visual quality matching the “*Seven Lines*” configuration. This way, the more numerous, lower quality “*Macular Cube*” images can be converted to the visual style of the “*Seven Lines*” preset, with the corresponding reduction in speckle noise and the enhancement in tissue visibility that is characteristic of this more intensive scan, allowing the generation of synthetic images to be used for over-sampling as if they were originally acquired with this configuration. Additionally, we trained another model to carry out the opposite conversion of “*Seven Lines*” images, conferring them the visual style and speckle noise of “*Macular Cube*” samples.

These models were trained for a maximum of 400 epochs, using Adam[10] as an optimiser with $\beta_1 = 0.5$, $\beta_2 = 0.999$ and a learning rate of $2e-4$. These were used to generate the synthetic images of the opposed class by applying them to the original training samples, as represented in Figure 3.

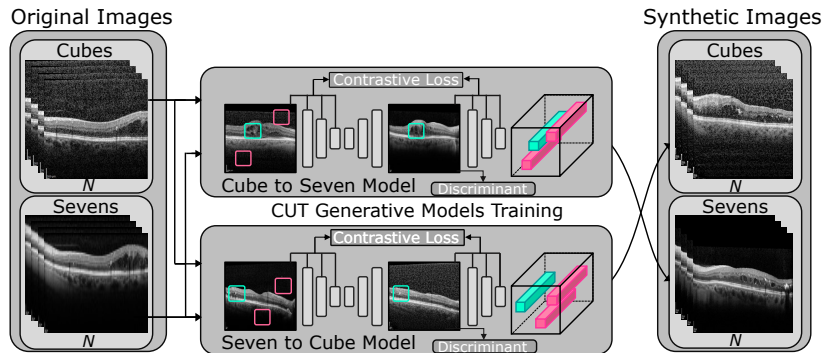


Fig. 3. Diagram showing the synthetic image generation methodology. By training two CUT generative models, we can then transform original “*Macular Cube*” and “*Seven Lines*” images into synthetic images of the opposed class.

3 Results and Discussion

To train and validate the CUT-based synthetic image generator models, we used 240 OCT slices acquired from different patients in accordance with the Declaration of Helsinki, approved by the local Ethics Committee of Investigation from A Coruña/Ferrol (2014/437) the 24th of November, 2014. The platform used to acquire the images was a Heidelberg SPECTRALIS[®] OCT scanner configured with the two aforementioned presets shown in Figure 1. In particular, 120 images belonged to the “*Macular Cube*” class with lower overall quality and resolution, while the remaining 120 were acquired with the “*Seven Lines*” preset. These images were resized to a resolution of 256×256 pixels and then used to train both of the CUT-GAN models. The loss curves for the 400 epochs of training are shown in Figure 4.

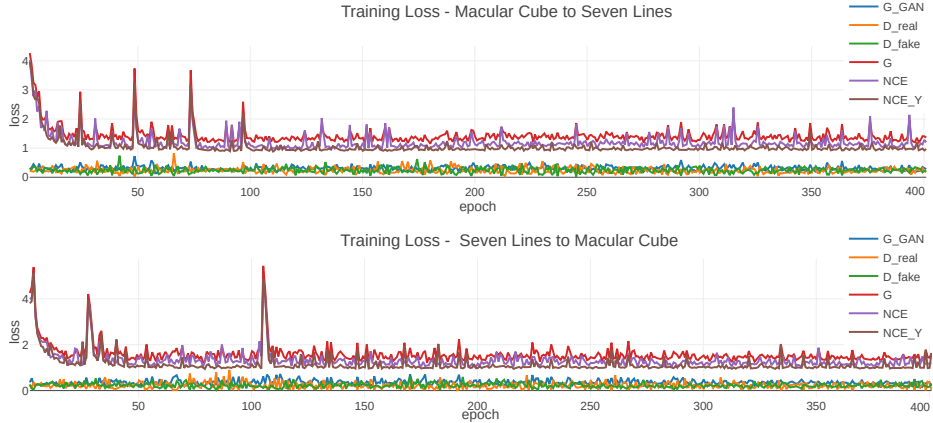


Fig. 4. Training losses for both generative models. G_GAN : generator GAN loss, D_real : discriminator loss for real images, D_fake : discriminator loss for fake images, G : generator loss, NCE : Noise Contrastive Estimation loss for images of the original class, NCE_Y : NCE loss for images of the target class.

To evaluate and assess the quality of the synthetic data, an experiment was performed using the Blind/Referenceless Image Spatial Quality Evaluator BRISQUE [14], an automatic image quality evaluator commonly used in medical imaging literature for similar purposes [2, 28, 27]. BRISQUE does not require a reference image to perform a comparison unlike other metrics such as Structural Similarity Index Measure or Peak Signal to Noise Ratio. Instead, when analysing a single image, it returns a score that is indicative of the perceptual quality of said image. The higher the perceived quality, the lower the BRISQUE score.

In the experiment, the quality score of every original image was assessed and compared to that of the synthetic ones. The original “*Cube*” and “*Seven*” images achieved an average BRISQUE score of 80.36 ± 25.05 and 42.42 ± 9.29

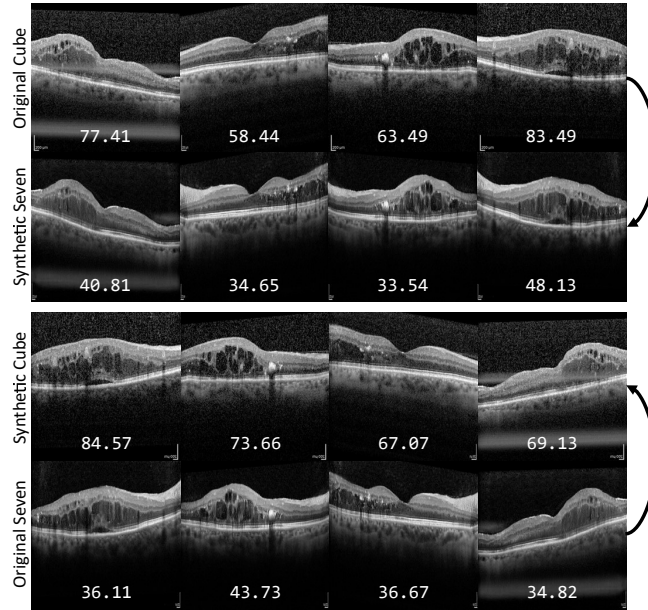


Fig. 5. Examples of original images and the resulting generated picture of the opposite class. *Top*: “Macular Cube” to “Seven Lines”. *Bottom*: “Seven Lines” to “Macular Cube”. Numbers in white indicate the BRISQUE score.

respectively, while the generated images were rated at 84.59 ± 15.47 and 42.91 ± 7.94 , correspondingly, to synthetic generated “Cube” and “Seven” images. Some examples of original images and their corresponding synthetic generated samples are displayed in Figure 5. These results show that the generative networks are able to mimic the visual features of the target classes whilst preserving the original tissue structure. Since the available dataset is unpaired, no reference image-based quality assessment can be performed.

The generative adversarial network training process involves the use of a discriminator that distinguishes between original and synthetic images. The aim of this discriminator is to guide the training process by providing a loss component which penalises generated images that do not mimic the visual features of the original images correctly. However, this discriminator is intentionally simple, in order to allow the generative model to progressively adjust during training. Furthermore, the training process forces the discriminator to progressively learn the visual features that distinguish original and synthetic images. This leaves this discriminator biased towards the training process, which aims to a relative stability in terms of losses, as can be seen in Figure 4. Because of its simplicity and bias, this discriminator is a poor candidate for assessing the separability of the synthetic generated images. In an effort to more objectively assess the validity of the synthetic samples, an independent separability test was performed. The aim of this separability test is to verify whether the synthetic generated images

display the visual features that characterise each of the presets. In this test, a classifier is first trained to classify the original images according to the visual features that they display, learning the characteristics that distinguish each preset. When tested on the synthetic generated images, these should be classified according to the visual features of the preset they are converted to, instead of those corresponding to the scanning preset that was used to acquire them. By using a Densely Connected Convolutional Network [7] architecture, which has demonstrated its advantages for classification tasks in medical imaging [16], we can achieve an objective validation of the separability of the synthetic data.

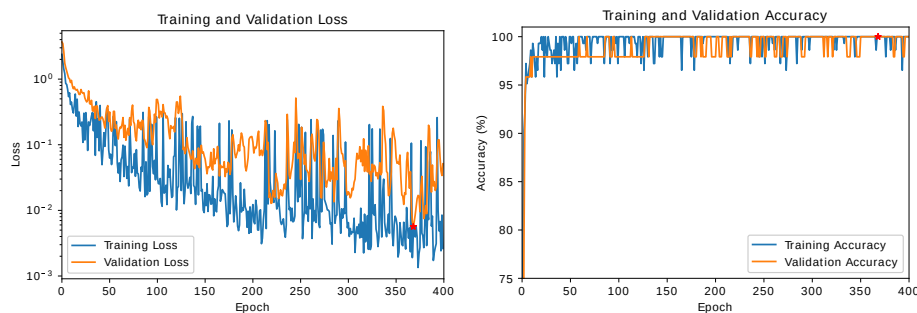


Fig. 6. Training and validation losses in logarithmic scale and accuracies for the DenseNet-121 classifier. The model with the lowest validation loss is marked with a red star.

In this separability test, a DenseNet-121 classifier was trained to discern between “*Macular Cube*” and “*Seven Lines*” images from the original dataset. This dataset was partitioned with 60% of the samples being used for training, 20% for validation and the remaining 20% to test the model. The model was trained for a maximum of 400 epochs on the training samples, and the checkpoint which performed best on the validation set was selected for testing. During this training, we used Adam [10] as an optimiser, with a learning rate of $2e-4$, $\beta_1 = 0.5$, and $\beta_2 = 0.999$. The training and validation loss and accuracy curves are displayed in Figure 6. The loss curves are represented in logarithmic scale in order to provide a better visualisation.

Afterwards, the synthetic images that were generated by the CUT-GAN models were assigned to their transferred class and tested with this classifier, comparing the results with those obtained with the test that used original images. This process, and the results that were obtained, are represented in Figure 7. These satisfactory results show that the generative models are able to synthesise images that can successfully display the visual characteristics of the target class.

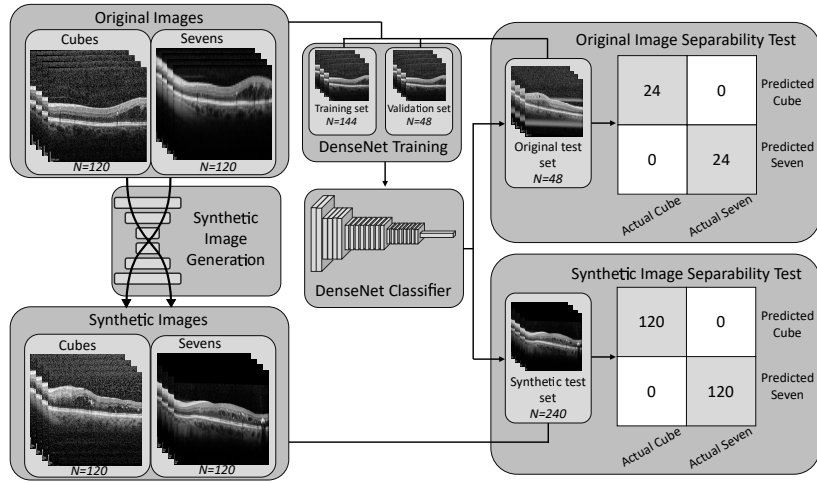


Fig. 7. Diagram describing the tests that were performed to assess the separability of the synthetic images, together with the resulting test confusion matrices.

4 Conclusions

Almost half of the population that suffers from a form of visual impairment is under-diagnosed or affected by a preventable condition. OCT imaging can be used to create CAD systems that help to diagnose and assess these pathologies. However, the necessary compromise between image quality and the amount of tissue that can be analysed in a single session leads to a scarcity of high quality data.

In this work, we present a fully automatic methodology for the mutual “style transfer” of OCT images taken from the two most widely used scanning presets, constituting the first example of such conversion in the literature. This method is able to transform noisy, low quality “*Macular Cube*” OCT scans into cleaner “*Seven Lines*”-quality scans while preserving tissue texture, as well as to perform the inverse transformation. The obtained test results show that these synthetic images achieve the visual features of their assigned class, with a very similar BRISQUE score when compared with original images. Additionally, the results that were produced by the separability test indicate that these synthetic generated images are clearly separable into their respective target classes. The ability to mutually transfer the style of multiple presets has the potential to produce multi-preset datasets with which to train more robust CAD systems. Moreover, the potential of this methodology is not limited to OCT imaging, as it is applicable to many other imaging techniques such as angiographies or retinographies.

As future work, our plans encompass the validation of this synthetic image generation methodology with human experts, verifying if ophthalmologists are able to distinguish the original images from the synthetic generated ones. Addi-

tionally, we plan to evaluate this generative methodology on screening tests by supplying single-preset datasets with synthetic generated images converted to other presets, assessing the benefits these may provide on the training of robust CAD systems designed for the screening of ocular pathologies.

References

1. Apostolopoulos, S., Salas, J., Ordóñez, J.L.P., Tan, S.S., Ciller, C., Ebnetter, A., Zinkernagel, M., Sznitman, R., Wolf, S., Zanet, S.D., Munk, M.R.: Automatically enhanced OCT scans of the retina: A proof of concept study. *Scientific Reports* **10**(1) (May 2020). <https://doi.org/10.1038/s41598-020-64724-8>
2. Chaabouni, A., Gaudeau, Y., Lambert, J., Moureaux, J.M., Gallet, P.: Subjective and objective quality assessment for h264 compressed medical video sequences. In: 2014 4th International Conference on Image Processing Theory, Tools and Applications (IPTA). pp. 1–5 (2014). <https://doi.org/10.1109/IPTA.2014.7001922>
3. Cheung, C.Y., Tang, F., Ting, D.S.W., Tan, G.S.W., Wong, T.Y.: Artificial intelligence in diabetic eye disease screening. *Asia-Pacific Journal of Ophthalmology* (2019). <https://doi.org/10.22608/apo.201976>
4. Fu, H., Cheng, J., Xu, Y., Wong, D.W.K., Liu, J., Cao, X.: Joint optic disc and cup segmentation based on multi-label deep network and polar transformation. *IEEE Transactions on Medical Imaging* **37**(7), 1597–1605 (Jul 2018). <https://doi.org/10.1109/tmi.2018.2791488>
5. Gende, M., De Moura, J., Novo, J., Charlón, P., Ortega, M.: Automatic segmentation and intuitive visualisation of the epiretinal membrane in 3d oct images using deep convolutional approaches. *IEEE Access* **9**, 75993–76004 (2021). <https://doi.org/10.1109/ACCESS.2021.3082638>
6. Gulshan, V., Peng, L., Coram, M., Stumpe, M.C., Wu, D., Narayanaswamy, A., Venugopalan, S., Widner, K., Madams, T., Cuadros, J., Kim, R., Raman, R., Nelson, P.C., Mega, J.L., Webster, D.R.: Development and validation of a deep learning algorithm for detection of diabetic retinopathy in retinal fundus photographs. *JAMA* **316**(22), 2402 (Dec 2016). <https://doi.org/10.1001/jama.2016.17216>
7. Huang, G., Liu, Z., Maaten, L.V.D., Weinberger, K.Q.: Densely connected convolutional networks. In: 2017 IEEE Conference on Computer Vision and Pattern Recognition (CVPR). pp. 2261–2269. IEEE (Jul 2017). <https://doi.org/10.1109/cvpr.2017.243>
8. Huang, Y., Lu, Z., Shao, Z., Ran, M., Zhou, J., Fang, L., Zhang, Y.: Simultaneous denoising and super-resolution of optical coherence tomography images based on generative adversarial network. *Optics Express* **27**(9), 12289 (Apr 2019). <https://doi.org/10.1364/oe.27.012289>
9. Kamalipour, A., Moghimi, S.: Macular optical coherence tomography imaging in glaucoma. *Journal of Ophthalmic and Vision Research* (Jul 2021). <https://doi.org/10.18502/jovr.v16i3.9442>
10. Kingma, D.P., Ba, J.: Adam: A method for stochastic optimization. In: Bengio, Y., LeCun, Y. (eds.) 3rd International Conference on Learning Representations, ICLR 2015, San Diego, CA, USA, May 7-9, 2015, Conference Track Proceedings (2015), <http://arxiv.org/abs/1412.6980>
11. Lee, J.H., Kim, Y.T., Lee, J.B., Jeong, S.N.: A performance comparison between automated deep learning and dental professionals in classification of dental implant systems from dental imaging: A multi-center study. *Diagnostics* **10**(11), 910 (Nov 2020). <https://doi.org/10.3390/diagnostics10110910>

12. Li, M., Idoughi, R., Choudhury, B., Heidrich, W.: Statistical model for oct image denoising. *Biomed. Opt. Express* **8**(9), 3903–3917 (Sep 2017). <https://doi.org/10.1364/BOE.8.003903>, <http://www.osapublishing.org/boe/abstract.cfm?URI=boe-8-9-3903>
13. Litjens, G., Kooi, T., Bejnordi, B.E., Setio, A.A.A., Ciompi, F., Ghafoorian, M., van der Laak, J.A., van Ginneken, B., Sánchez, C.I.: A survey on deep learning in medical image analysis. *Medical Image Analysis* **42**, 60–88 (2017). <https://doi.org/https://doi.org/10.1016/j.media.2017.07.005>
14. Mittal, A., Moorthy, A.K., Bovik, A.C.: No-reference image quality assessment in the spatial domain. *IEEE Transactions on Image Processing* **21**(12), 4695–4708 (2012). <https://doi.org/10.1109/TIP.2012.2214050>
15. de Moura, J., Novo, J., Ortega, M.: Deep feature analysis in a transfer learning-based approach for the automatic identification of diabetic macular edema. In: 2019 International Joint Conference on Neural Networks (IJCNN). IEEE (Jul 2019). <https://doi.org/10.1109/ijcnn.2019.8852196>
16. Nugroho, K.A.: A Comparison of Handcrafted and Deep Neural Network Feature Extraction for Classifying Optical Coherence Tomography (OCT) Images. In: 2018 2nd International Conference on Informatics and Computational Sciences (ICICoS). pp. 1–6 (2018). <https://doi.org/10.1109/ICICOS.2018.8621687>
17. Park, T., Efros, A.A., Zhang, R., Zhu, J.Y.: Contrastive learning for unpaired image-to-image translation. In: *Computer Vision – ECCV 2020*. pp. 319–345. Springer International Publishing, Cham (2020). https://doi.org/10.1007/978-3-030-58545-7_19
18. Puliafito, C.A., Hee, M.R., Lin, C.P., Reichel, E., Schuman, J.S., Duker, J.S., Izatt, J.A., Swanson, E.A., Fujimoto, J.G.: Imaging of macular diseases with optical coherence tomography. *Ophthalmology* **102**(2), 217–229 (Feb 1995). [https://doi.org/10.1016/s0161-6420\(95\)31032-9](https://doi.org/10.1016/s0161-6420(95)31032-9), [https://doi.org/10.1016/s0161-6420\(95\)31032-9](https://doi.org/10.1016/s0161-6420(95)31032-9)
19. Schmitt, J.: Optical coherence tomography (OCT): a review. *IEEE Journal of Selected Topics in Quantum Electronics* **5**(4), 1205–1215 (1999). <https://doi.org/10.1109/2944.796348>
20. Shorten, C., Khoshgoftaar, T.M.: A survey on image data augmentation for deep learning. *Journal of Big Data* **6**(1) (Jul 2019). <https://doi.org/10.1186/s40537-019-0197-0>, <http://dx.doi.org/10.1186/s40537-019-0197-0>
21. Ting, D.S.W., Cheung, C.Y.L., Lim, G., Tan, G.S.W., Quang, N.D., Gan, A., Hamzah, H., Garcia-Franco, R., Yeo, I.Y.S., Lee, S.Y., Wong, E.Y.M., Sabanayagam, C., Baskaran, M., Ibrahim, F., Tan, N.C., Finkelstein, E.A., Lamoureux, E.L., Wong, I.Y., Bressler, N.M., Sivaprasad, S., Varma, R., Jonas, J.B., He, M.G., Cheng, C.Y., Cheung, G.C.M., Aung, T., Hsu, W., Lee, M.L., Wong, T.Y.: Development and validation of a deep learning system for diabetic retinopathy and related eye diseases using retinal images from multiethnic populations with diabetes. *JAMA* **318**(22), 2211 (Dec 2017). <https://doi.org/10.1001/jama.2017.18152>
22. Ting, D.S.W., Pasquale, L.R., Peng, L., Campbell, J.P., Lee, A.Y., Raman, R., Tan, G.S.W., Schmetterer, L., Keane, P.A., Wong, T.Y.: Artificial intelligence and deep learning in ophthalmology. *British Journal of Ophthalmology* **103**(2), 167–175 (Oct 2018). <https://doi.org/10.1136/bjophthalmol-2018-313173>
23. Triolo, G., Rabiolo, A.: Optical coherence tomography and optical coherence tomography angiography in glaucoma: diagnosis, progression, and correlation with functional tests. *Therapeutic Advances in Ophthalmology* **12**, 251584141989982 (Jan 2020). <https://doi.org/10.1177/2515841419899822>

24. Vujosevic, S., Toma, C., Villani, E., Muraca, A., Torti, E., Florimbi, G., Leporati, F., Brambilla, M., Nucci, P., De Cilla, S.: Diabetic macular edema with neuroretinal detachment: Oct and oct-angiography biomarkers of treatment response to anti-vegf and steroids. *Acta diabetologica* **57**(3), 287–296 (2020). <https://doi.org/10.1007/s00592-019-01424-4>
25. World Health Organization: World Report on Vision. World Health Organization (2019), <https://www.who.int/publications/i/item/9789241516570>
26. Xu, M., Tang, C., Hao, F., Chen, M., Lei, Z.: Texture preservation and speckle reduction in poor optical coherence tomography using the convolutional neural network. *Medical Image Analysis* **64**, 101727 (Aug 2020). <https://doi.org/10.1016/j.media.2020.101727>
27. Yu, S., Dai, G., Wang, Z., Li, L., Wei, X., Xie, Y.: A consistency evaluation of signal-to-noise ratio in the quality assessment of human brain magnetic resonance images. *BMC Medical Imaging* **18**(1) (May 2018). <https://doi.org/10.1186/s12880-018-0256-6>
28. Zhang, Z., Dai, G., Liang, X., Yu, S., Li, L., Xie, Y.: Can signal-to-noise ratio perform as a baseline indicator for medical image quality assessment. *IEEE Access* **6**, 11534–11543 (2018). <https://doi.org/10.1109/access.2018.2796632>